AIP Journal of Applied Physics

Capping layer-tailored interface magnetic anisotropy in ultrathin Co2FeAl films

M. Belmeguenai, M. S. Gabor, T. Petrisor Jr., F. Zighem, S. M. Chérif, and C. Tiusan

Citation: Journal of Applied Physics **117**, 023906 (2015); doi: 10.1063/1.4905688
View online: http://dx.doi.org/10.1063/1.4905688
View Table of Contents: http://scitation.aip.org/content/aip/journal/jap/117/2?ver=pdfcov
Published by the AIP Publishing

Articles you may be interested in

Co2FeAl Heusler thin films grown on Si and MgO substrates: Annealing temperature effect
J. Appl. Phys. **115**, 043918 (2014); 10.1063/1.4863398

Quantifying perpendicular magnetic anisotropy at the Fe-MgO(001) interface
Appl. Phys. Lett. **102**, 122410 (2013); 10.1063/1.4798291

Tunnel magnetoresistance effect in magnetic tunnel junctions with epitaxial Co2FeAl0.5Si0.5 Heusler electrodes on MgO (110) single substrates
J. Appl. Phys. **111**, 07C718 (2012); 10.1063/1.3678586

Magnetic properties of Fe0.4Mn0.6/Co2FeAl bilayers grown on GaAs by molecular-beam epitaxy
J. Appl. Phys. **110**, 093904 (2011); 10.1063/1.3657780

Magnetic anisotropies and magnetization reversal of the Co 2 Cr 0.6 Fe 0.4 Al Heusler compound
J. Appl. Phys. **100**, 103904 (2006); 10.1063/1.2387059

MIT LINCOLN LABORATORY CAREERS

Discover the satisfaction of innovation and service to the nation

- Space Control
- Air & Missile Defense
- Communications Systems & Cyber Security
- Intelligence, Surveillance and Reconnaissance Systems
- Advanced Electronics
- Tactical Systems
- Homeland Protection
- Air Traffic Control

LINCOLN LABORATORY
MASSACHUSETTS INSTITUTE OF TECHNOLOGY

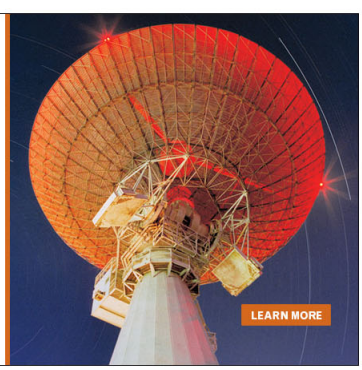

[This article is copyrighted as indicated in the article. Reuse of AIP content is subject to the terms at: http://scitation.aip.org/termsconditions. Downloaded to] IP: 193.50.135.4 On: Sun, 17 May 2015 06:05:57

Capping layer-tailored interface magnetic anisotropy in ultrathin Co_2FeAl films

M. Belmeguenai,[1,a)] M. S. Gabor,[2,b)] T. Petrisor, Jr.,[2] F. Zighem,[1] S. M. Chérif,[1] and C. Tiusan[2,3]
[1]*LSPM (CNRS-UPR 3407), Université Paris 13, Sorbonne Paris Cité, 99 Avenue Jean-Baptiste Clément, 93430 Villetaneuse, France*
[2]*Center for Superconductivity, Spintronics and Surface Science, Department of Physics and Chemistry, Technical University of Cluj-Napoca, Str. Memorandumului No. 28, RO-400114 Cluj-Napoca, Romania*
[3]*Institut Jean Lamour, CNRS, Lorraine Université, BP 70239, F-54506 Vandoeuvre, France*

(Received 4 November 2014; accepted 29 December 2014; published online 12 January 2015)

Co_2FeAl (CFA) thin films of various thicknesses ($2\,nm \leq d \leq 50\,nm$) have been grown on (001) MgO single crystal substrates and then capped with Cr, V, and Ta. Their magnetic and structural properties have been studied by x-ray diffraction (XRD), vibrating sample magnetometry, and broadband microstrip ferromagnetic resonance (MS-FMR). The XRD revealed that the films are epitaxial with the cubic [001] CFA axis normal to the substrate plane and that the chemical order varies from the B2 phase to the A2 phase when decreasing the thickness. The deduced lattice parameters showed that the Cr-capped films exhibit a larger tetragonal distortion, as compared with the films capped with V or Ta. The presence of magnetic dead layers has been observed in CFA samples capped with V and Ta but not in the case of the Cr-capped ones. The effective magnetization, deduced from the fit of MS-FMR measurements, increases (decreases) linearly with the CFA inverse thickness ($1/d$) for the Cr-capped (Ta-capped) films while it is constant for the V-capped ones. This allows quantifying the perpendicular surface anisotropy coefficients of $-0.46\,erg/cm^2$ and $0.74\,erg/cm^2$ for Cr and Ta-capped films, respectively. Moreover, the fourfold and the uniaxial anisotropy fields, measured in these films, showed different trends with a respect to the CFA inverse thickness. This allows inferring that a non-negligible part of the fourfold magnetocrystalline term is of interfacial origin. © *2015 AIP Publishing LLC*. [http://dx.doi.org/10.1063/1.4905688]

I. INTRODUCTION

Perpendicular magnetic anisotropy (PMA) is one of the key magnetic thin film properties for operating modern spintronics devices,[1] such as spin transfer torque magnetic random access memories (STT-MRAM). Here, the integration of materials with PMA allows low critical current densities (J_{c0}) and high thermal stability.[2] Recently, strong PMA in ferromagnetic (FM) thin films, Co, CoFe, and CoFeB when interfaced with an oxide, has been demonstrated.[3–6] Using first principles calculations, the anatomy of the PMA in these systems has been explained via the hybridization of the O 2p and the FM (e.g. Fe) 3d orbitals, together with a degeneracy lift induced by the spin-orbit coupling (SOC). The main advantage of the PMA obtained via the hybridization phenomena at FM transition metal alloy/oxide interface is related to the possibility of avoiding the adjunction of large SOC elements like Pd or Pt (as alloy constituents or adjacent layers). This latter strategy would have a detrimental effect on both Gilbert damping and spin polarization of the FM material.

Among the ferromagnetic materials largely studied in spintronics, the full Heusler alloy Co_2FeAl (CFA) is one of the most promising. It has a high Curie temperature (1000 K) and, following theoretical predictions, a half-metallic character of the spin-split band structure. Moreover, it has been demonstrated to provide giant tunneling magnetoresistance ratios (360% at room temperature (RT))[8] when used as ferromagnetic electrode in magnetic tunnel junctions. This furthermore proves the CFA significant potential for practical applications. Moreover, due to its small damping values[9] and long FM coherent length, the CFA is suitable for magnonic[10] devices. Typically, the CFA thin films exhibit in-plane magnetization due to the thin film shape anisotropy. However, we recently showed that CFA thin films (thickness down to 10 nm) grown on MgO substrates exhibit a strong negative perpendicular anisotropy (reinforcing the in-plane easy axis). This turns out to be a pure interface contribution.[9] Therefore, it is of great interest for both fundamental and technological reasons to investigate the magnetic behavior of the CFA ultrathin films (thickness down to 2 nm) grown on MgO and to point-out the role of capping layer materials on the interfacial anisotropy, for manufacturing CFA films with PMA. Thus, the aim of this paper is to investigate the effect of the capping layer (three different transition metals: Cr, V, and Ta) on the structural and magnetic properties of CFA ultrathin films.

The experimental strategy employed in this paper was a complex analysis of the correlation between the structural and magnetic (static and dynamic) properties. Therefore, the x-ray diffraction (XRD), the ferromagnetic resonance in microstrip line (MS-FMR) under in-plane applied magnetic fields, combined with the vibrating sample magnetometry

a)belmeguenai.mohamed@univ-paris13.fr
b)mihai.gabor@phys.utcluj.ro

 © 2015 AIP Publishing LLC

[This article is copyrighted as indicated in the article. Reuse of AIP content is subject to the terms at: http://scitation.aip.org/termsconditions. Downloaded to] IP: 193.50.135.4 On: Sun, 17 May 2015 06:05:57

(VSM) allowed us to correlate structural and magnetic properties of CFA ultrathin films grown on MgO substrates and capped with different layers. Our results demonstrate that the presence of the interface anisotropy as well as its sign depends on the cap layer, offering the possibility for versatile samples design with skillfully tuned magnetic properties: PMA and in-plane anisotropy.

II. SAMPLES PREPARATION AND EXPERIMENTAL METHODS

The CFA films were grown on MgO(001) single-crystal substrates using a magnetron sputtering system with a base pressure lower than 3×10^{-9} Torr. Prior to the deposition of the CFA films, a 5 nm thick MgO buffer layer was grown at RT by rf sputtering from a MgO polycrystalline target under an Argon pressure of 15 mTorr. Next, the CFA films, with variable thicknesses ($d = 50$, 30, 10, 7.5, 5, 3, and 2 nm), were deposited at RT by dc sputtering under an Argon pressure of 1 mTorr, at a rate of 0.1 nm/s. Finally, the CFA films were capped with 5 nm thick layers of different nature (Cr, V, and Ta). After the growth of the stack, the structures were *ex-situ* annealed at 450 °C during 60 min in vacuum (pressure lower than 3×10^{-8} Torr).

For the dynamic measurements, we used the MS-FMR technique, where the sample is mounted on a 0.5 mm microstrip line connected to the microwave generator and to a lock-in amplifier to derive the field first derivative of the absorbed power. During the measurement, the external magnetic field H was applied in various directions with a respect to the [110] axis of the CFA. The magnetization at saturation and the hysteresis loops have been measured with VSM and the structural properties were investigated by XRD.

III. RESULTS AND DISCUSSIONS

A. Structural properties

X-ray diffraction experiments have been performed for all the CFA films in order to determine their crystal structure. Figure 1(a) shows the typical x-ray 2θ-ω (out-of-plane) diffraction patterns recorded for the Ta-capped samples. The corresponding in-plane diffraction patterns around the (022) Co_2FeAl reflection peak are shown on Figure 1(b). These measurements revealed that all the samples exhibit only the (002) and (004) peaks of CFA, in addition to the peak corresponding to the MgO substrate (not shown here). This indicates a (00l) textured growth of the films. Φ-scan measurements (not shown here) confirmed the epitaxial growth of the films with the expected CFA (001)[110]//MgO(001)[100] epitaxial relation. The (002) superlattice peak is characteristic of the B2 phase of CFA, characterized by disorder between Fe and Al while Co atoms occupy regular sites. Therefore, the absence of this peak is a signature of the A2 phase in which Fe, Al, and Co occupy randomly the atomic sites. Since the (004) reflection is a fundamental one corresponding to the cubic CFA structure, the integrated peak intensity ratio I(002)/I(004) represents the measure of the degree of order on Co sites. This ratio, shown in Figure 1(c), increases with the CFA

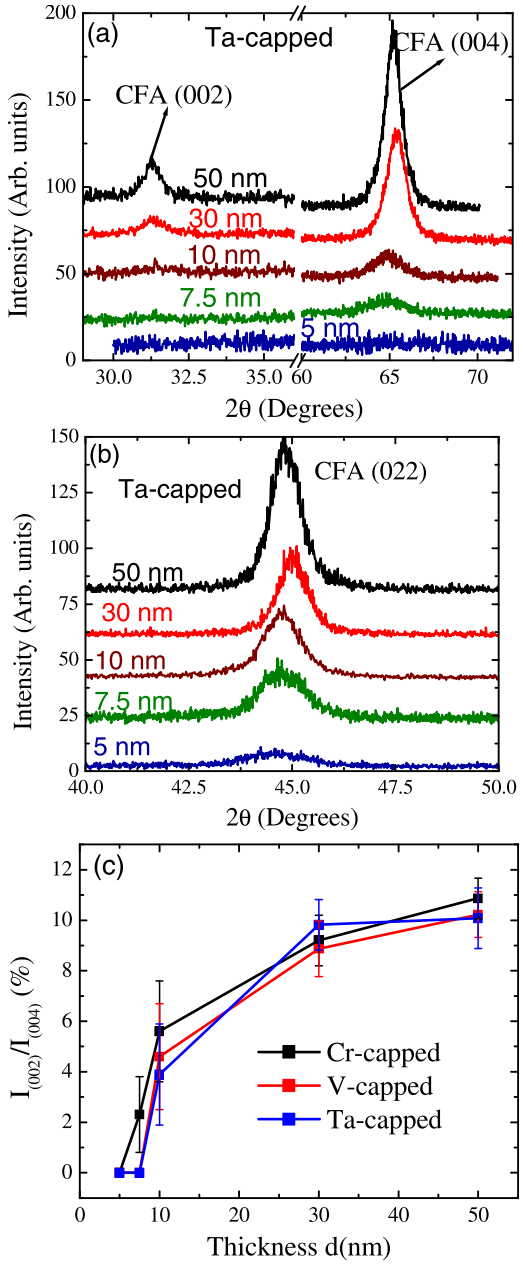

FIG. 1. (a) X-ray 2θ-ω (out-of-plane) diffraction patterns and (b) in-plane diffraction patterns around (220) for Ta-capped Co_2FeAl of different thicknesses. (c) Evolution of the integral intensities of the (002) and (004) Co_2FeAl peaks $I(002)/I(004)$ with respect to the Co_2FeAl films thickness capped with Cr, V, and Ta.

thickness suggesting a monotonous enhancement of the chemical order from the A2 towards the B2 phase.

Using the XRD measurements, we evaluated the out-of-plane and the in-plane lattice parameters, as shown on Figure 2. Due to the overlap of the Cr capping reflections, in the case of the Cr-capped samples, the estimation of the lattice parameters was quite difficult and the error bar is significant. For $d < 5$ nm, the estimation of the lattice parameter was not possible due to the very low signal-to-noise ratio. The dashed line represents the corresponding lattice parameter value for the bulk $L2_1$ ordered CFA phase.[11] For all the samples, the thinner films ($d = 5$ nm) experience a relatively strong tetragonal distortion. As the thickness increases, this distortion

[This article is copyrighted as indicated in the article. Reuse of AIP content is subject to the terms at: http://scitation.aip.org/termsconditions. Downloaded to] IP: 193.50.135.4 On: Sun, 17 May 2015 06:05:57

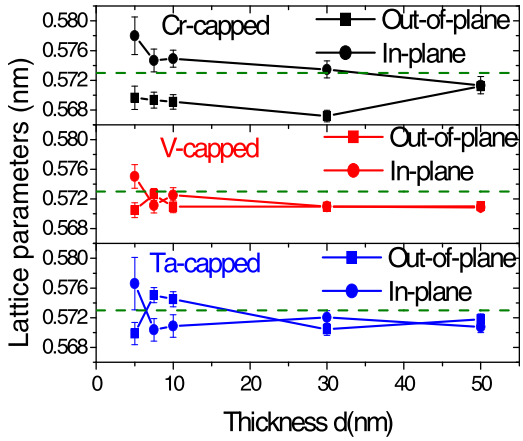

FIG. 2. Thickness evolution of out-of-plane and in-plane lattice parameters of Co_2FeAl films capped with Cr, V, and Ta.

relaxes: for the film thickness around 30 nm, the out-of-plane and the in-plane lattice parameters show practically identical values. This tetragonal distortion is more pronounced for the Cr-capped samples and is most probably attributed to residual strains resulting from the growth mode; the Cr capping layer shows an epitaxial growth on CFA, which is not the case for the Ta and V capping materials.

B. Magnetic properties

All the measurements presented here were performed at room temperature using a vibrating sample magnetometer for the static characterization and a home-made MS-FMR setup[9] for the dynamic magnetic investigations. The g value, which determines the gyromagnetic factor (γ), the magnetic anisotropy, the effective magnetization, and the exchange stiffness constant are precisely accessible by the MS-FMR technique, through the study of the frequency variation versus the amplitude and the direction of the in-plane applied magnetic field. Therefore, the magnetic parameters of CFA thin films of various thicknesses and capped with different materials were accurately derived at room temperature from MS-FMR measurements. Their variation versus the CFA thickness will be discussed below.

1. Static characterization

For all the studied films, the hysteresis loops were obtained by VSM with an in-plane magnetic field applied along various orientations φ_H with a respect to the [110] CFA axis. Figure 3 shows the representative behaviors of 10 nm thick CFA films capped with three different layers. The observed shape mainly depends on the field orientation, in agreement with the expected characteristics of the magnetocrystalline anisotropy. As confirmed below, in all the studied samples, this anisotropy consists of the superposition of a fourfold and a uniaxial term showing parallel easy axes: this common axis coincides with one of the ⟨110⟩ crystallographic directions of the CFA phase. It results that if an orientation (such as $\varphi_H = 0$: related to [110]) is the easiest (square hysteresis loops), the perpendicular

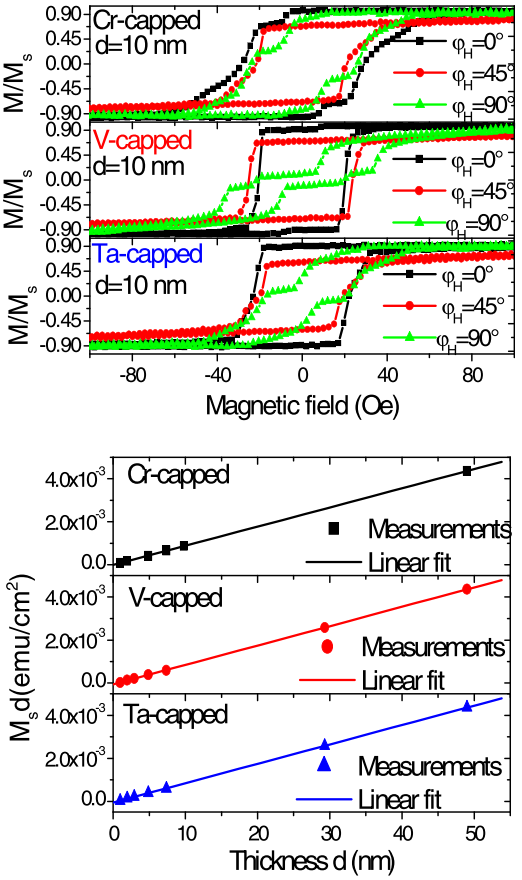

FIG. 3. VSM hysteresis loops of the 10 nm Cr, V, and Ta-capped Co_2FeAl thin films. The magnetic field is applied parallel to the film surface at various angles (φ_H) with a respect to the [110] CFA axis and thickness dependences of the saturation magnetic moment per unit area for the Cr, V, and Ta-capped Co_2FeAl thin films.

direction ($\varphi_H = 90°$: related to [1–10]) is the less easy (two steps reversal).

Figure 3 also shows the CFA thickness dependences of the saturation magnetic moment per unit area for the three kinds of samples. This thickness dependence of the magnetic moment is used to determine the magnetization at saturation and the magnetic dead layer: The slope gives the saturation magnetization, while the horizontal axis intercept gives the extent of the dead layer.

This saturation magnetization is determined to be 890 ($4\pi M_s \approx 11.18$ kOe), 874 ($4\pi M_s \approx 11$ kOe), and 885 emu/cm^3 ($4\pi M_s \approx 11.12$ kOe) for Cr, V, and Ta-capped films, respectively. The magnetic dead layer thickness is 0.5 and 0.7 nm, for the V and Ta-capped films, whereas it is nearly zero for Cr-capped samples. The magnetic dead layer is most likely the result of the intermixing at the CFA/capping interface, which is negligible in the case of Cr capping.

2. Dynamic characterization

The MS-FMR spectra measured for all the samples with an in-plane magnetic field applied at different directions φ_H with a respect to the [110] CFA axis (parallel to one of the MgO substrate edges) revealed the existence of the uniform precession mode. For the thickest film (50 nm), it was possible to observe the first perpendicular

[This article is copyrighted as indicated in the article. Reuse of AIP content is subject to the terms at: http://scitation.aip.org/termsconditions. Downloaded to] IP: 193.50.135.4 On: Sun, 17 May 2015 06:05:57

standing spin wave mode (PSSW). For the thinner films, the PSSW modes are not detected due to their high frequencies over-passing the available bandwidth (0–20 GHz). The typical in-plane field dependence of the resonance frequencies of the uniform and PSSW modes is shown in Figure 4(a) for the 50 nm Cr-capped films for $\varphi_H = 0°$ (easy axis) and $\varphi_H = 45°$ (hard axis). The typical MS-FMR angular dependence of the uniform precession mode resonance field at 10 GHz driven frequency for 3, 5, and 10 nm CFA thick films capped with Cr, V, and Ta layers is shown on Figure 4(b). This angular behavior of the resonance field is governed by the superposition of a small uniaxial, traduced by different resonance fields at 0° (180°) and 90° (270°), and a dominated fourfold anisotropies having parallel easy axes: their common axis coincides with one of the substrate edges and, consequently, with the ⟨110⟩ crystallographic direction of CFA. The epitaxial symmetry properties agree with the principal directions of the fourfold contribution suggesting a magnetocrystalline origin of the fourfold anisotropy. The corresponding field dependence of the resonance frequencies recorded for the applied field along the easy axis of CFA thin films is shown on Figure 4(c).

The experimental data presented here have been analyzed considering the model described in Ref. 9, where the resonance expression of the uniform precession mode and for the PSSW modes assuming in-plane applied magnetic fields is given by

$$F_n{}^2 = \left(\frac{\gamma}{2\pi}\right)^2 \left[H\cos(\varphi_H - \varphi_M) + \frac{2K_4}{M_s}\cos 4(\varphi_M - \varphi_4) + \frac{2K_u}{M_s}\cos 2(\varphi_M - \varphi_u) + \frac{2A_{ex}}{M_s}\left(\frac{n\pi}{d}\right)^2 \right] \times \left[H\cos(\varphi_H - \varphi_M) + 4\pi M_{eff} + \frac{K_4}{2M_s}\left(3 + \cos 4(\varphi_M - \varphi_4)\right) + \frac{K_u}{M_s}\left(1 + \cos 2(\varphi_M - \varphi_u)\right) + \frac{2A_{ex}}{M_s}\left(\frac{n\pi}{d}\right)^2 \right], \quad (1)$$

where $(\gamma/2\pi) = g \times 1.397 \times 10^6$ Hz/Oe is the gyromagnetic factor, n is the index of the PSSW mode, and A_{ex} is the exchange stiffness constant.

In the above expression, φ_M represents the in-plane (referring to the [110] CFA axis) angle defining the direction of the magnetization M_s. φ_u and φ_4 define the angles between the planar uniaxial easy axis and the planar fourfold easy axis with a respect to this [110] axis, respectively. K_u, K_4, and $K_\perp$ are the in-plane uniaxial, the fourfold, and the out-of-plane uniaxial anisotropy constants, respectively. We define $H_u = \frac{2K_u}{M_s}$ and $H_4 = \frac{4K_4}{M_s}$ as the in-plane uniaxial and the fourfold anisotropy fields and we introduce the effective magnetization $M_{eff} = H_{eff}/4\pi$ obtained by

$$4\pi M_{eff} = H_{eff} = 4\pi M_s - \frac{2K_\perp}{M_s} = 4\pi M_s - H_\perp. \quad (2)$$

As it was experimentally observed, the effective perpendicular anisotropy term $K_\perp$ as well as K_u and K_4 is thickness dependent. $K_\perp$ describes an effective perpendicular anisotropy term which is written as $K_\perp = K_{\perp v} + K_{\perp s}/d$, where $K_{\perp s}$ refers to the perpendicular anisotropy term of the interfacial energy density. In the same manner, we write $H_u = H_{uV} + \frac{2K_{us}}{dM_s}$ and $H_4 = H_{4V} + \frac{4K_{4s}}{dM_s}$, where K_{4s} and K_{us} are the interfacial fourfold and uniaxial anisotropy constants.

By fitting the data in Figure 4(a) to the above presented model, the gyromagnetic factor (γ), exchange stiffness constant (A_{ex}), and the effective magnetization ($4\pi M_{eff}$) are extracted. The fitted γ and A_{ex} values are found to be constant across the different samples and equal to 29.2 GHz/T and 1.45 μ erg/cm, respectively. This exchange constant value is in good agreement with that indicated in Ref. 12.

Interestingly, the extracted effective magnetization from the MS-FMR measurements, shown in Figure 5(a) follows different behaviors with a respect to the CFA thickness, depending on the cap layer material. It shows a linear variation versus the inverse CFA thickness for Cr and Ta-capped films while it seems to be thickness independent (the average value of $4\pi M_{eff}$ is equal to 10.2 kOe) in the case of V-capped ones. The linear fit of the measurements allows for determining the perpendicular surface anisotropy constants values: $K_{\perp s} = -0.46$ erg/cm^2 and $K_{\perp s} = 0.74$ erg/cm^2 for Cr and Ta-capped films, respectively. Notice the opposite sign of these constants: it reinforces the in-plane anisotropy axis in the case of Cr, while it favors a perpendicular anisotropy easy axis for Ta-capped films. The $4\pi M_{eff}$ value when d tends to infinity, equal to 10.6 kOe and 10 kOe, respectively, for Cr and Ta-capped films, is slightly different from the $4\pi M_s$ mentioned above, suggesting the existence of a volume perpendicular anisotropy in the range of 0.6–1 kOe depending, of the cap layer material. The value of the surface perpendicular anisotropy constant, in the case of the Ta capped films, is in agreement with that of the Si/Ta/CFA/MgO structures.[13] As shown in Ref. 13, this value of the interface anisotropy constant decreases to about 0.48 erg/cm^2 at annealing temperature of 350 °C.

The origin of PMA at 3d metal-alloy/MgO interface is attributed, from first principle calculations, to the hybridization of the O2*p* and metal-alloy *3d* orbitals.[14–16] Since it was shown that under- or over-oxidation at the 3d metal-alloy/MgO interface can strongly influence the interfacial magnetic anisotropy,[14–16] the quality of the CFA/MgO interface is extremely important. The quality of the CFA/MgO interface might be capping layer dependent, for example, thorough capping layer diffusion or lattice strain.[17] Moreover, the effective magnetization, in the case of the Cr-capped films, increases linearly with the lattice parameter as shown in Figure 5(b). This experimental result may originate from the anisotropy induced by the lattice strain. Furthermore, an

[This article is copyrighted as indicated in the article. Reuse of AIP content is subject to the terms at: http://scitation.aip.org/termsconditions. Downloaded to] IP: 193.50.135.4 On: Sun, 17 May 2015 06:05:57

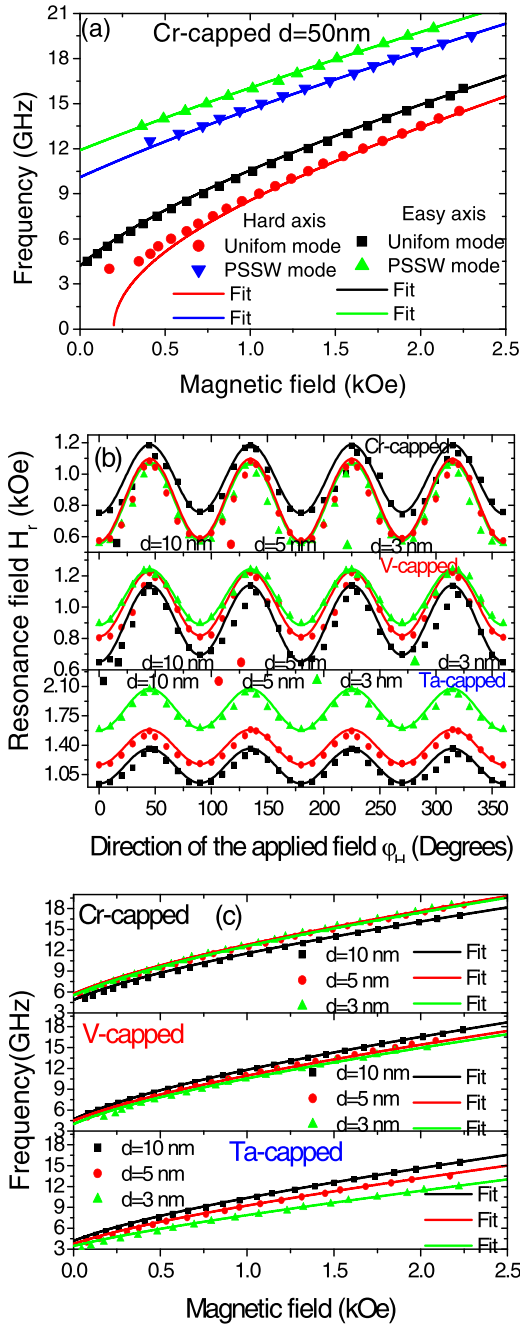

FIG. 4. (a) Field dependence of the resonance frequency of the uniform precession and of the first perpendicular standing spin wave (PSSW) mode of 50 nm Cr-capped Co_2FeAl films. (b) Angular dependence of the resonance field at 10 GHz driven frequency and (c) easy axis field dependence of the resonance frequency of the uniform precession of Cr, V, and Ta-capped Co_2FeAl films of thickness d. The magnetic field is applied in the film plane. The fits are obtained using Eq. (1).

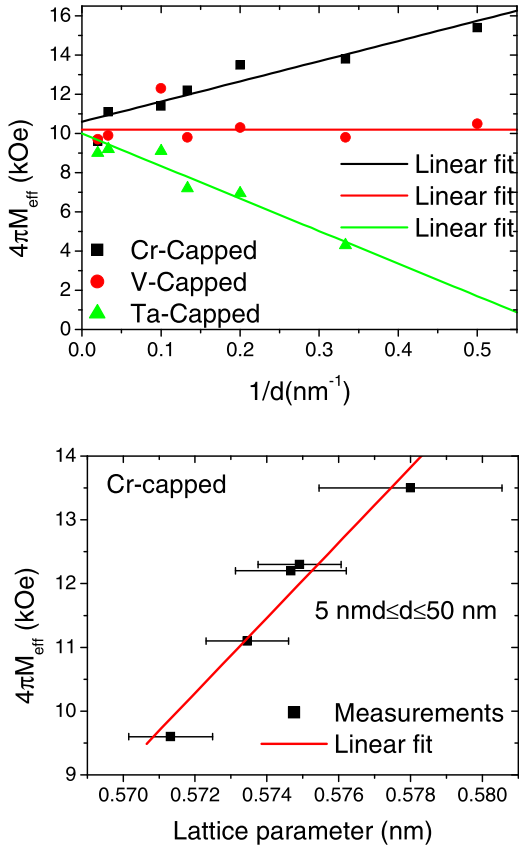

FIG. 5. (a) Thickness dependence and (b) lattice parameter dependence of the effective magnetization ($4\pi M_{eff}$) extracted from the fit of FMR measurements of Cr, V, and Ta-capped Co_2FeAl films. The solid lines are linear fits.

additional contribution to the interfacial magnetic anisotropy might be related to the CFA/capping layer interface[6,7] through the electronic structure modification of the CFA surface in the presence of the capping layer. Therefore, the origin of this interface anisotropy is most probably a combine effect of the above mentioned mechanisms, involving both the CFA/MgO and the CFA/capping layer interface. Depending on the CFA/capping layer interface contribution, the resulting interface anisotropy is reinforced or reduced or even cancelled like in the case of the V.

The uniaxial and the fourfold anisotropy fields, deduced from the fit of FMR data, are presented in Figure 6 as CFA inverse thickness. For the thicker films ($d \geq 5$ nm), the fourfold anisotropy fields vary linearly with $1/d$ for the Cr and Ta-capped films giving rise to fourfold anisotropy surface constants $K_{4s} = 1.7 \times 10^{-2}$ erg/cm^2, $K_{4s} = 1.1 \times 10^{-2}$ erg/cm^2 for the Cr and Ta-capped films, respectively. The volume fourfold anisotropy field deduced from the linear fit of the experimental data presented in Figure 6 is 400 Oe, suggesting that the most contribution to the fourfold term is of magnetocrystalline origin. It is worth to mention that a similar behavior (over the film range of 115–10 nm), where Cr-capped films have higher fourfold interface anisotropy compared to the Ta-capped ones, has been observed for CFA films annealed at 600 °C.[9] For the film thickness below 5 nm, the fourfold anisotropy fields decrease linearly with $1/d$ for the Cr and V-capped films maybe due to the degradation of films quality for lower thicknesses.

The uniaxial anisotropy field (H_u) does not show a clear behaviour versus CFA inverse thickness, even for larger values of the film thickness ($d > 5$ nm). In a first approximation, we can consider that this field is thickness independent and having a mean value around 9 Oe for all the samples. This uniaxial anisotropy could be induced during the sample growth. However, in our previous work[9] on Ta-capped samples annealed at 600 °C, we observed a clear $1/d$ linear behaviour of H_u suggesting an interfacial contribution to this uniaxial anisotropy. Owing to that, one might presume that a linear behaviour of

[This article is copyrighted as indicated in the article. Reuse of AIP content is subject to the terms at: http://scitation.aip.org/termsconditions. Downloaded to] IP: 193.50.135.4 On: Sun, 17 May 2015 06:05:57

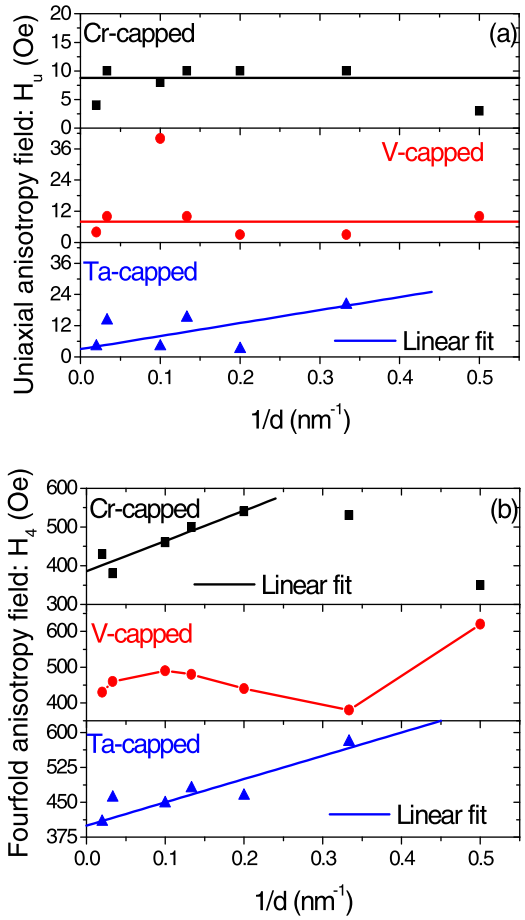

FIG. 6. Thickness dependence of (a) the uniaxial (H_u) and (b) the fourfold anisotropy fields (H_4) extracted from the fit of FMR measurements of Cr, V, and Ta-capped Co_2FeAl films. The solid lines in (a) refer to the fit with a constant mean value (for Cr and V-capped films) or to the linear fit (Ta-capped films). For (b), the solid lines refer to the linear fits (for Cr and T-capped films) or are used as guide for eyes (for V-capped films).

H_u could be present for the Ta-capped samples but could be hidden by its small amplitude at 450 °C annealing temperature. If we assume that the thickness dependence of H_u for the Ta-capped films is linear, the derived uniaxial surface anisotropy constant K_{us} of 2.2×10^{-3} erg/cm^2 is extremely weak compared to that observed for samples annealed at 600 °C ($K_{us} = 1.79 \times 10^{-2}$ erg/cm^2). This increase in H_4 is presumably related to the B2 ⇒A2 phase transition observed through x-ray diffraction as the thickness increases. For the film thickness below 5 nm, the fourfold anisotropy fields decrease linearly with $1/d$ for the Cr and V-capped films maybe due to the degradation of films crystalline quality for lower thicknesses.

IV. CONCLUSION

Co_2FeAl films of various thicknesses ($2\,\text{nm} \leq d \leq 50\,\text{nm}$), capped with different materials (Cr, V, and Ta) and annealed at 450 °C, were prepared by sputtering on (001) MgO substrates. They show an epitaxial growth with a chemical order changing from B2 to A2 phase, as thickness decreases. The lattice parameter's thickness dependence investigation revealed that the CFA films present a strong tetragonal distortion. This has been found to be capping layer dependent and to relax when the film's thickness is increased. The VSM hysteresis loops obtained for different in-plane applied magnetic field orientations revealed that depending on the applied field direction, two or one jump switching occurs due to the superposition of uniaxial and fourfold anisotropy. The CFA thickness dependences of the saturation magnetic moment per unit area allow to determine a mean value of the magnetization at saturation of 885 emu/cm^3 and a dead layer thickness of 0.5 and 0.7 nm for the V and Ta-capped films, respectively, whereas it is nearly zero for Cr-capped samples. The MS-FMR technique has been furthermore used to study the dynamic properties and the magnetic anisotropy. The in-plane anisotropy has been found to present two contributions, showing a fourfold and a uniaxial symmetry. The fourfold in-plane anisotropy fields show a thickness dependence behavior due to the interface anisotropy, while the uniaxial anisotropy field does not show clear thickness dependence. The effective magnetization deduced from the fit of MS-FMR measurements increases (decreases) linearly with $1/d$ for the Cr-capped (Ta-capped) films, while it is constant for the V-capped ones.

ACKNOWLEDGMENTS

This work has been partially supported by the Exploratory Research Project, SPINTAIL PN-II-ID-PCE-2012-4-0315, No. 23/29.08.2013, by POS CCE ID. 574, code SMIS-CSNR 12467, and by TUCN—MADSPIN Research Project.

[1]A. Brataas, A. D. Kent, and H. Ohno, Nature Mater. **11**, 372 (2012).
[2]S. Mangin, D. Ravelosona, J. A. Katine, M. J. Carey, B. D. Terris, and E. E. Fullerton, Nature Mater. **5**, 210 (2006).
[3]S. Ikeda, K. Miura, H. Yamamoto, K. Mizunuma, H. D. Gan, M. Endo, S. Kanai, J. Hayakawa, F. Matsukura, and H. Ohno, Nature Mater. **9**, 721 (2010).
[4]S. Monso, B. Rodmacq, S. Auffret, G. Casali, F. Fettar, B. Gilles, B. Dieny, and P. Boyer, Appl. Phys. Lett. **80**, 4157 (2002).
[5]A. Manchon, C. Ducruet, L. Lombard, S. Auffret, B. Rodmacq, B. Dieny, S. Pizzini, J. Vogel, V. Uhlir, M. Hochstrasser, and G. Panaccione, J. Appl. Phys.**104**, 043914 (2008).
[6]H. Yamamoto, J. Hayakawa, K. Miura, K. Ito, H. Matsuoka, S. Ikeda, and H. Ohno, Appl. Phys. Express **5**, 053002 (2012).
[7]C. H. Lambert, A. Rajanikanth, T. Hauet, S. Mangin, E. E. Fullerton, and S. Andrieu, Appl. Phys. Lett. **102**, 122410 (2013).
[8]W. H. Wang, H. Sukegawa, and K. Inomata, Phys. Rev. B **82**, 092402 (2010).
[9]M. Belmeguenai, H. Tuzcuoglu, M. S. Gabor, T. Petrisor, Jr., C. Tiusan, D. Berling, F. Zighem, T. Chauveau, S. M. Chérif, and P. Moch, Phys. Rev. B **87**, 184431 (2013).
[10]H. Ulrichs, B. Lenk, and M. Münzenberg, Appl. Phys. Lett. **97**, 092506 (2010).
[11]H. J. Elmers, S. Wurmehl, G. H. Fecher, G. Jakob, C. Felser, and G. Schönhense, Appl. Phys. A **79**, 557 (2004).
[12]M. Belmeguenai, H. Tuzcuoglu, M. S. Gabor, T. Petrisor, Jr., C. Tiusan, F. Zighem, T. Chauveau, S. M. Chérif, and P. Moch, J. Appl. Phys. **115**, 043918 (2014).
[13]M. S. Gabor, T. Petrisor, Jr., C. Tiusan, and T. Petrisor, J. Appl. Phys. **114**, 063905 (2013).
[14]H. X. Yang, M. Chshiev, B. Dieny, J. H. Lee, A. Manchon, and K. H. Shin, Phys. Rev. B **84**, 054401 (2011).
[15]A. Hallal, H. X. Yang, B. Dieny, and M. Chshiev, Phys. Rev. B **88**, 184423 (2013).
[16]J. Okabayashi, J. W. Koo, H. Sukegawa, S. Mitani, Y. Takagi, and T. Yokoyama, Appl. Phys. Lett. **105**, 122408 (2014).
[17]K. H. He, Y. P. Feng, and J. S. Chen, J. Appl. Phys. **111**, 07C109 (2012).

[This article is copyrighted as indicated in the article. Reuse of AIP content is subject to the terms at: http://scitation.aip.org/termsconditions. Downloaded to] IP: 193.50.135.4 On: Sun, 17 May 2015 06:05:57